SPANDIDOS PUBLICATIONS

INTERNATIONAL JOURNAL OF ONCOLOGY 53: 579-591, 2018

Early synergistic interactions between the HPV16-E7 oncoprotein and 17β-oestradiol for repressing the expression of Granzyme B in a cervical cancer model

J. ANTONIO MUNGUÍA-MORENO[1*], JOSÉ DÍAZ-CHAVÉZ[2*], ENRIQUE GARCÍA-VILLA[1], M. ESTELA ALBINO-SANCHEZ[1], DANIEL MENDOZA-VILLANUEVA[3,8], RODOLFO OCADIZ-DELGADO[1], JOSÉ BONILLA-DELGADO[4], ARMANDO MARÍN-FLORES[1], ENOC M. CORTÉS-MALAGÓN[4], ELIZABETH ALVAREZ-RIOS[1], ALFREDO HIDALGO-MIRANDA[5], AYKUT ÜREN[6], HAYDAR ÇELIK[6], PAUL F. LAMBERT[7] and PATRICIO GARIGLIO[1]

[1]Department of Genetics and Molecular Biology, Centre for Research and Advanced Studies of the National Polytechnic Institute, México City 07360; [2]Biomedical Unit for Cancer Research, National Autonomous University of Mexico/National Institute of Cancer, México City 14080, México; [3]Laboratory of Cell and Developmental Signalling, National Cancer Institute at Frederick, Frederick, MD 21702, USA; [4]Research Unit of Genetics and Cancer, Juárez Hospital, México City 07760; [5]Department of Oncogenomics, National Institute of Genomic Medicine, México City 14610, México; [6]Department of Oncology, Lombardi Comprehensive Cancer Centre, Georgetown University Medical Centre, Washington, DC 20057; [7]McArdle Laboratory for Cancer Research, University of Wisconsin School of Medicine and Public Health, Madison, WI 53706, USA

Received September 28, 2017; Accepted February 23, 2018

DOI: 10.3892/ijo.2018.4432

Abstract. Although high-risk human papillomavirus (HR-HPV) infection has a prominent role in the aetiology of cervical cancer (CC), sex steroid hormones may also be involved in this process; however, the cooperation between oestrogen and HR-HPV in the early stages of cervical carcinogenesis is poorly understood. Since 17β-oestradiol (E_2) and the HPV type 16-E7 oncoprotein induce CC in transgenic mice, a microarray analysis was performed in the present study to generate global gene expression profiles from 2-month-old FVB (non-transgenic) and K14E7 (transgenic) mice who were left untreated or were treated for 1 month with E_2. Upregulation of cancer-related genes that have not been previously reported in the context of CC, including glycerophosphodiester phosphodiesterase domain containing 3, interleukin 1 receptor type II, natriuretic peptide type C, MGAT4 family member C, lecithin-retinol acyltransferase (phosphatidylcholine-retinol-O-acyltransferase) and glucoside xylosyltransferase 2, was observed. Notably, upregulation of the serine (or cysteine) peptidase inhibitor clade B member 9 gene and downregulation of the Granzyme gene family were observed; the repression of the Granzyme B pathway may be a novel mechanism of immune evasion by cancer cells. The present results provide the basis for further studies on early biomarkers of CC risk and synergistic interactions between HR-HPV and oestrogen.

Correspondence to: Dr Patricio Gariglio, Department of Genetics and Molecular Biology, Centre for Research and Advanced Studies of the National Polytechnic Institute, 2508 National Polytechnic Institute Avenue, San Pedro Zacatenco, Gustavo A. Madero, México City 07360, México
E-mail: vidal@cinvestav.mx

[*]Contributed equally

Present address: [8]TOMA Biosciences, Inc., 303 Vintage Park Drive, Suite 210, Foster City, CA 94404, USA

Key words: human papillomavirus type 16-E7, 17β-oestradiol, microarrays, carcinogenesis, K14E7, Granzyme B

Introduction

Cervical cancer (CC) development is associated with infection with high-risk human papillomavirus (HR-HPV) types, predominantly HPV16 and HPV18 (1). CC accounts for nearly 300,000 mortalities worldwide every year (2), representing a medical challenge in developing countries, and HPV16 is the most prevalent viral subtype that is responsible for ~50% of CC cases (3). The HR-HPV oncoproteins E6 and E7 are involved in the induction and maintenance of CC; however, other co-factors are necessary for CC development. For example, in transgenic mice, it was found that E7 cooperates with 17β-oestradiol (E_2) to induce high-grade dysplasia, *in situ* carcinoma and CC (4). Additionally, it has been shown that E_2 contributes not only to the onset, but also to the persistence and malignant progression of CC in K14E7 transgenic mice (5); notably, E_2 fails to promote dysplasia or CC in K14E7 mice that lack oestrogen receptors(6).

These studies suggest that E_2 has a prominent role together with the E7 protein in cell transformation and tumour development during cervical carcinogenesis (7). However, little is known about the causal and temporal associations between genotypic and phenotypic alterations, particularly associated with E7 plus E_2, in the induction of cervical malignant lesions, as well as the potential role of the cellular stress response in the earliest stages of cervical carcinogenesis (8).

In the present study, global gene expression profiling and RT-qPCR analysis were performed to determine the mRNA expression landscape of cervical tissues obtained from 2-month-old mice, in order to identify genes regulated by HPV16-E7 and E_2 that may serve a role in early cervical carcinogenesis. Differentially expressed cancer-related genes were identified that have a synergistic effect at the transcriptional level on factors associated with cellular movement, cancer, metabolism, apoptosis, cellular growth and proliferation, as well as the regulation of cell morphology and inflammatory responses. Of particular note was the downregulation of the Granzyme B (GrB) pathway as a possible mechanism of immune evasion. GrB/perforin-induced cell death is one of the main mechanisms used by cytotoxic T lymphocytes (CTLs) and natural killer (NK) cells to destroy allogenic, virus-infected and tumour cells (9). However, it is known that GrB has extracellular functions and is expressed in non-immune cells, including smooth muscle cells, chondrocytes and keratinocytes (10,11), as well as in the prostate cancer PC-3 and DU145 cell lines (12), and that the activation of GrB could be potentially harmful to cells producing GrB. In this regard, it has been shown that the activation of GrB by ultraviolet A (UVA) radiation in keratinocytes is partially responsible for the reduction of viable cells (13). Furthermore, in prostate cancer cells, resveratrol has been shown to induce the expression of GrB, which is correlated with enhanced apoptosis and increased radiosensitivity of the PCA cells (12). As GrB pathway components are often elevated in chronic inflammation-associated and/or degenerative pathologies (14), and as GrB produced in keratinocytes and other non-immune cells is active and partially responsible for the induction of death in these cells (12,13), the inhibition of GrB pathway components may suppress the activation of the GrB pathway in CC cells, thereby inducing neoplasia. In addition, the upregulation of the natural inhibitor of GrB, the serine protease inhibitor SERPINB9 [also known as protease inhibitor-9 (PI-9)], can also mediate the inhibition of endogenous and exogenous GrB secretion by immune cells (15,16). The present study opens the possibility of assessing and validating novel early-risk biomarkers and therapeutic targets for CC, enabling a better understanding of the molecular mechanisms by which HPV16-E7 and E_2 can lead to CC development.

Materials and methods

Mouse models and hormone treatment. The K14E7 and FVB mouse models have been previously described (4). Briefly, mice were obtained from the mouse repository located at National Cancer Institute at Frederick campus (Frederick, MD, USA). The K14E7 transgenic mice were generated and maintained in the FVB/N inbred strain and used as transgenic heterozygotes harbouring overlapping HPV16 E6 and E7 open reading frames (ORFs) spanning nucleotides 79-883 with a TTL in the E6 gene to preclude E6 expression. Persistent oestrogen administration and E7 expression were sufficient to produce high-grade cervical dysplasia and invasive cervical malignancies (17). For this study, four groups were created: FVB (not transgenic, not treated, control group), FVB+E_2 (not transgenic, treated group), K14E7 (transgenic, untreated group) and K14E7+E_2 (transgenic, treated group). The mice were housed and treated according to guidelines from the Association for Assessment and Accreditation of Laboratory Animal Care International and the National Institutes of Health Guide for the Care and Use of Laboratory Animals (publication no. 8023, revised 1978). The euthanasia procedure via use of a CO_2 chamber was followed according to the American Veterinary Medical Association's Guidelines for the Euthanasia of Animals (2013 edition).

All experiments and procedures were approved by the Research Unit for Laboratory Animal Care Committee (NOM-062-ZOO-1999; Unit for the Production and Experimentation of Laboratory Animals, The Centre for Research and Advanced Studies of the National Polytechnic Institute, México City, México). The environmental conditions for the mice included free access to food/water with a standard diet of LabDiet®, a 12:12 light:dark cycle, a room temperature of 25˚C and 30% humidity, with housing in Super Mouse 750™ Micro-Isolator® cages in groups of 4-5 mice. Female, 1-month-old, virgin transgenic and non-transgenic mice, weighing 12-13 g, were dorsally implanted with continuous release pellets under the skin, which delivered 0.05 mg E_2 (Innovative Research of America, Sarasota, FL, USA) over 60 days. After 1 month of treatment, the mice, weighing 13-15 g, were sacrificed at 2 months of age. Control and treatment groups were formed using 20 to 24 mice in each.

Tissue procurement and histopathology. Untreated or treated K14E7 hemizygous and non-transgenic FVB control virgin female mice were sacrificed by CO_2 chamber. All specimens were fixed in 4% paraformaldehyde at 4˚C overnight and embedded in paraffin. Sections were deparaffinized and rehydrated as previously described (18). Serial sections were cut (at 5-μm thickness) and stained with haematoxylin and eosin (H&E) at room temperature (10 min haematoxylin and 2 min eosin).

Tissue procurement and microarray sample processing. Untreated or treated K14E7 hemizygous and non-transgenic FVB control virgin female mice were sacrificed by CO_2 chamber. Cervical biopsy samples were immediately stored in RNAlater® solution (Thermo Fisher Scientific, Inc., Waltham, MA, USA) at 4˚C overnight. Tissues were recovered from RNAlater solution with sterile forceps, quickly blotted to remove excess solution and immediately snap-frozen in liquid nitrogen. Total RNA was extracted from snap-frozen tissues using standard procedures with TRIzol reagent (Invitrogen; Thermo Fisher Scientific, Inc.). In total, 2 pooled samples from 3 mice were used to avoid variability and to identify biomarkers for the early stages of carcinogenesis in a population of K14E7 mice treated with E_2, as recommended by previous studies (19-21). Total RNA collected from 6 female mice from each group was pooled. RNA quantity and quality were assessed on an Agilent 2100 Bioanalyzer (Agilent Technologies, Inc., Santa Clara, CA, USA). RNA samples with an RNA integrity score of >8.0 were further processed for

Table I. Primer sequences.

Gene name	Forward primers	Reverse primers
Gapdh (mouse)	5'-GTG GAG TCA TAC TGG AAC ATG TAG-3'	5'-AAT GGT GAA GGT CGG TGT G-3'
Gzmb (mouse)	5'-CAT GTC CCC CGA TGA TCT C-3'	5'-AAG AGA GCA AGG ACA ACA CTC-3'
Gzmc (mouse)	5'-CTC CTC CTT AGC CTT GAT GTT G-3'	5'-CGA GAC AAA TTC GTG CTA ACA G-3'
Gzmd (mouse)	5'-GAA GCC TCC ACA GTA TAT CCT G-3'	5'-CCT GAT TCT CCT GAC CCT ACT-3'
Gzme (mouse)	5'-CCT CCA CAG TAT CTC CTA TTA CCT-3'	5'-ACC AGT CCT GAT TCT CCT GA-3'
Gzmf (mouse)	5'-CCA TTA TCT TTC ACA AAC CTC ACA C-3'	5'-TGG AGC AGA GGA GAT CAT CG-3'
Gzmg (mouse)	5'-ACT CCA TAA GCT AGG TTG TCA C-3'	5'-CTA TTC CAA GAC CAC GCA GAT-3'
Gdpd3 (mouse)	5'-GTT CAT CCA TCC ACA GCG AA-3'	5'-CCT TTT GTC TCC ATC CCT GA-3'
Lrat (mouse)	5'-AAG ACA GCC GAA GCA AGA C-3'	5'-GCG AAC ACT TTG TGA CTT ACT G-3'
Nppc (mouse)	5'-CAT TGC GTT GGA GGT GTT TC-3'	5'-GGT CTG GGA TGT TAG TGC AG-3'
Mgat4c (mouse)	5'-ACT GAT GAA AGT CCA ATT GTG AG-3	5'-CAC CAA CTT AAT TCT GAA CGC T3'
Cyp2e1 (mouse)	5'-GCC TCA TTA CCC TGT TTC CC-3	5'-TTC CAG GAG TAC AAG AAC AAG G-3'
Il1r2 (mouse)	5'-CCT TCC AGC CTC AAT TCA GAT-3	5'-TGC TTT CAC CAC TCC AAC AG-3'
Stat5a (mouse)	5'-GCT CTC ATC CAG GTC AAA CTC-3	5'-TGC CCT CAA CCT CAC TAC A-3'
Eomes (mouse)	5'-CCA GAA CCA CTT CCA CGA AA-3	5'-CGG CAC CAA ACT GAG ATG A-3'
Gxylt2 (mouse)	5'-TGG CCC CAG AGC ATG AAA -3'	5'-CCG GGC AAA GCG ACT GTA-3'
Serpinb9 (mouse)	5'-GTG CCA TTT CCT TCA GAC AG-3	5'-GAA GTC CCT GCC TTG TAC AG-3'
SERPINB9B (human)	5'-AGT GAG AAG CGA CTG GAA AG-3'	5'-CTG TTC TCC TGT GAG CAT CTC-3'
GZMB (human)	5'-CAG AGA CTT CTG ATC CCA GAT-3	5'-TCC TGA GAA GAT GCA ACC AAT -3'
B2M (human)	5'-ACC TCC ATG ATG CTG CTT AC-3	5'-GGA CTG GTC TTT CTA TCT CTT GT-3'

Gzm, Granzyme; *Cyp2e1*, cytochrome P450 family 2 subfamily e polypeptide 1; *Gdpd3*, glycerophosphodiester phosphodiesterase domain containing 3; *Il1r2*, interleukin 1 receptor type II; *Lrat*, lecithin-retinol acyltransferase (phosphatidylcholine-retinol-O-acyltransferase); *Mgat4c*, MGAT4 family member C; *Nppc*, natriuretic peptide type C; *Gxylt2*, glucoside xylosyltransferase 2; *GZMB*, Granzyme B; *Eomes*, eomesodermin; *Serpinb9*, serine (or cysteine) peptidase inhibitor clade B member 9; *Stat5*, signal transducer and activator of transcription 5; *B2M*, β2-microglobulin level.

microarray analysis. cDNA synthesis, amplification and gene expression profiling were performed according to the manufacturer's protocols (Affymetrix® WT Sense Target Labelling assay; Thermo Fisher Scientific, Inc.). Affymetrix microarray experiments were performed in triplicate for each group in the GeneChip Mouse Gene 1.0 ST Array platform.

Analysis of array data. Signal intensities from each array were analysed using Partek Genomic Suite version 6.4 (Partek, Inc., Chesterfield, MO, USA). Raw intensity values for the probes were normalized using robust multiarray analysis background correction. Two-way analysis of variance (ANOVA) was performed to identify differentially expressed genes. Genes with statistically significant differences in expression levels ($P<0.05$) and a fold change of ≥1.5 and ≤-1.5 were included in the final set of differentially expressed genes. To identify the biological processes altered by E7 and/or E_2, Ingenuity Pathway Analysis (IPA; https://www.qiagenbioinformatics.com/products/ingenuity-pathway-analysis/; Ingenuity Systems, Redwood City, CA, USA), a bioinformatics tool for visualizing expression data in the context of Kyoto Encyclopaedia of Genes and Genomes-defined biological pathways (http://www.genome.jp/kegg/) was used.

Relative mRNA quantification by reverse transcription-quantitative polymerase chain reaction (RT-qPCR) and data analysis using the $2^{-\Delta\Delta Cq}$ method. RNA isolated by TRIzol reagent (Invitrogen; Thermo Fisher Scientific, Inc.) from 6 mice from each group (K14E7, FVB, K14E7+E_2 and FVB+E_2) was purified, and RNA quality determined by electrophoresis on a 2% agarose gel, with visualization of ribosomal RNA by ethidium bromide staining. RNA was quantified by spectrophotometric analysis at 260 and 280 nm. cDNA synthesis was performed using the Maxima First Strand cDNA Synthesis kit according to the manufacturer's protocols (Thermo Fisher Scientific, Inc.). RT-qPCR was performed using an Applied Biosystems 7300 instrument and a DNA Master SYBR Green I kit (both Thermo Fisher Scientific, Inc.). Templates were amplified using 45 cycles of a 3-step PCR protocol, which included 30 sec of denaturation at 95˚C, 30 sec of primer-dependent annealing at 60˚C and 30 sec of template-dependent elongation at 72˚C. Each gene-specific RNA was quantified in triplicate by qPCR, and mRNA ratios relative to the house-keeping gene GAPDH were calculated for standardization of gene expression levels across samples using the $2^{-\Delta\Delta Cq}$ method (22). All primer sequences and product sizes are shown in Table I.

Cell culture and transfection. Human foreskin primary keratinocytes (HFKs) were obtained from the American Type Culture Collection (Manassas, VA, USA) and cultured at 37˚C in a humidified atmosphere with 5% CO_2 in Dulbecco's

modified Eagle's medium:F12 supplemented with 0.18 mM adenine (Sigma-Aldrich®; Merck KGaA, Darmstadt, Germany), 0.1 μg/ml hydrocortisone (Sigma-Aldrich; Merck KGaA), 100X Human Keratinocyte Growth Supplement (Thermo Fisher Scientific, Inc.), 2% foetal bovine serum (Gibco; Thermo Fisher Scientific, Inc.) and an antibiotic-antimycotic mixture (Invitrogen; Thermo Fisher Scientific, Inc.). The cells were transfected with the HPV16-E7 oncogene using Attractene® reagent (Qiagen GmbH, Hilden, Germany) according to the manufacturer's recommended protocols. The cells were seeded in 6-well plates ($3x10^5$ cells/well), and the next day, the cells were transfected with a mixture of 4.5 μl Attractene/well and 1.2 μg plasmid (PCDNA3 HPV-16E7) per well. To obtain transient and stable transfected cell lines, the expression of β2-microglobulin was used as an internal control of gene expression in the qPCR assay. Cells were selected and maintained in growth media containing 200 mg/ml geneticin (G418; Invitrogen; Thermo Fisher Scientific, Inc.).

Immunohistochemistry and immunofluorescence procedures. Cervical tissue sections were fixed in 4% paraformaldehyde overnight at 4˚C for immunohistochemical staining. Tissues were cut into 5-μm sections with a microtome and placed on electro-charged slides (Van-Wessel, Querétaro, México) and preserved using GVA mount solution (Zymed®; Thermo Fisher Scientific, Inc.). Protein detection for immunohistochemistry was conducted using the Mouse/Rabbit PolyDetector HRP/DAB Detection system® (Bio SB, Santa Barbara, CA, USA), according to the manufacturer's protocols, and HRP-conjugated anti-rat antibodies. The samples were incubated at 4˚C overnight with primary antibodies against Ki-67 (cat. no. BSB 5713; 1:100 dilution; Bio SB), $p16^{INK4a}$ (cat. no. sc-468; 1:100 dilution; Santa Cruz Biotechnology, Inc., Dallas, TX, USA), Granzyme B (GZMB; cat. no. AB4059; 1:100 dilution; Abcam, Cambridge, MA, USA) or PI-9 (cat. no. sc-57531; 1:100 dilution; Santa Cruz Biotechnology, Inc.). Anti-rabbit HRP-conjugated antibodies (1:200 dilution; cat. no. A0545; Sigma-Aldrich; Merck KGaA) were used as secondary antibodies for the detection of proteins. Following immunohistochemical procedures, the tissues were counterstained with haematoxylin (10 min haematoxylin and 2 min eosin) at room temperature and mounted using GVA mount solution (Zymed; Thermo Fisher Scientific, Inc.). For immunofluorescence, cervical tissue sections were rinsed in 1X PBS and blocked for 2 h at 4˚C with 1X PBS supplemented with 0.3% Triton X-100 and 1% bovine serum albumin (Sigma-Aldrich; Merck KGaA). Next, the sections were washed three times with 1X PBS and incubated for 1 h at 37˚C with the aforementioned primary antibodies against GZMB or PI-9. The sections were then incubated with a fluorescein isothiocyanate (FITC)-labelled secondary antibody (rabbit; 1:50 dilution; cat. no. 65-6111; Zymed; Thermo Fisher Scientific, Inc.) for 30 min at room temperature. The sections were then rinsed as aforementioned, counterstained with propidium iodide (30 min at room temperature) and mounted using Vectashield® (Vector Laboratories, Inc., Burlingame, CA, USA). The stained sections were examined by confocal microscopy using a Leica TCS SP2 (Leica Microsystems, Inc., Buffalo Grove, IL, USA). Captured images were imported into Adobe Photoshop CS6 (Adobe Systems, Inc., San Jose, CA, USA) to generate maximum projections.

UV irradiation of HFKs. UVC irradiation was performed with a 1300 Series Class II, Type A2 Biological Safety Cabinet (Thermo Fisher Scientific, Inc.). HFKs were grown at 37˚C in a humidified atmosphere with 5% CO_2 in DMEM:F12 media supplemented with 0.18 mM adenine (Sigma-Aldrich; Merck KGaA), 0.1 μg/ml hydrocortisone (Sigma-Aldrich; Merck KGaA), 4 μg/ml insulin (Gibco; Thermo Fisher Scientific, Inc.), 20 ng/ml recombinant epidermal growth factor (PeproTech, Inc., Rocky Hill, NJ, USA), 5% foetal bovine serum (Gibco; Thermo Fisher Scientific, Inc.) and an antibiotic-antimycotic mixture (Invitrogen®). HFKs were irradiated with UVC radiation for 30 sec in the absence of medium. Following the addition of DMEM:F12-HFK medium, HFKs were cultured for 24 h prior to harvesting.

Statistical analysis. For all microarray data comparisons, ANOVA with Tukey's honest significant difference post hoc test was performed using Partek Genomics Suite® 6.6 Software (Affymetrix; Thermo Fisher Scientific, Inc). For all RT-qPCR data comparisons a one-way ANOVA with Bonferroni correction was used, performed in GraphPad Prism 5 (Graphpad Software, Inc., La Jolla, CA, USA). $P<0.05$ was considered to indicate a statistically significant difference.

Results

Histopathological characterization and detection of $p16^{INK4a}$ and proliferating cell nuclear antigen (PCNA) biomarker expression in low-grade cervical lesions in K14E7 transgenic mice. H&E staining of cervical tissue sections from 2-month-old mice from the FVB, FVB+E_2, K14E7 and K14E7+E_2 groups showed that only the K14E7+E_2 group developed low-grade lesions corresponding to cervical intraepithelial neoplasia grade I (CIN-I) (H&E; Fig. 1). Histopathology of the exocervical tissues of FVB (non-transgenic) mice demonstrated normal stratified squamous epithelium (H&E-FVB; Fig. 1), with sporadic expression of $p16^{INK4a}$ and basal PCNA expression in the epithelial basal layer ($p16^{INK4a}$-FVB and PCNA-FVB; Fig. 1). Histopathology of the exocervical tissues of the E_2-treated FVB mice demonstrated moderately hyperproliferative squamous epithelium (arrows, H&E-FVB+E_2; Fig. 1), with similar sporadic expression of $p16^{INK4a}$ as the untreated FVB mice, but with a higher PCNA expression in the epithelial basal layer, as expected with E_2 treatment (arrows, $p16^{INK4a}$-FVB+E_2 and PCNA-FVB+E_2; Fig. 1). In K14E7 mice, wider stratified basal and middle epithelial layers were observed (H&E-K14E7; Fig. 1). As expected with high-risk HPV-associated lesions (23-25), $p16^{INK4a}$ expression was increased in these samples compared with that in samples from FVB mice (arrows, $p16^{INK4a}$-K14E7; Fig. 1). Additionally, an even signal for PCNA expression along the basal layer and a hyperproliferative stratified squamous epithelium in the exocervical tissues was observed (arrows, PCNA-K14E7; Fig. 1). Notably, in the E_2-treated K14E7 mice, the development of mild dysplasia, indicated by the presence of epithelial cells with large and extended nuclei in the basal and middle layers of the exocervical tissues (arrows, Fig. 1), accompanied with infiltration of mixed inflammatory cells (neutrophils and lymphocytes) was observed (dotted arrows, H&E-K14E7+E_2; Fig. 1). Similar to that in K14E7 mice, the expression of $p16^{INK4a}$ in the E_2-treated

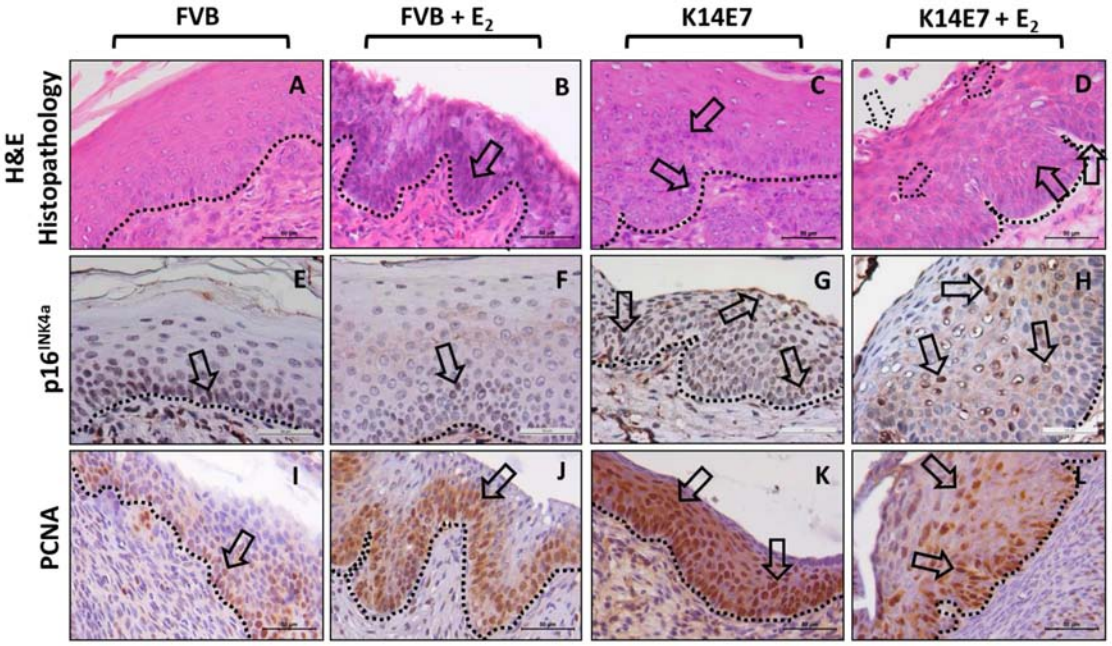

Figure 1. Histopathology of murine cervical tissues, and immunohistochemical detection of $p16^{INK4a}$ and PCNA biomarkers. Images correspond to cross-sections of exocervical epithelium from 2-month-old mice. H&E-FVB: Exocervical tissues of non-transgenic (FVB) mice showing normal stratified squamous epithelium. H&E-FBV+E_2: Exocervical tissues with moderately hyperproliferative squamous epithelial (arrow) in the FVB mice treated with E_2. H&E-K14E7: Exocervical tissues of K14E7 transgenic mice showing a wider stratified basal and middle epithelial layers (arrows). H&E-K14E7+E_2: Development of mild dysplasia, indicated by the presence of epithelial cells with large and extended nuclei and immature cells in the middle and basal layers (arrows). In addition, infiltration of mixed inflammatory cells (mainly neutrophils and lymphocytes; dotted arrows) can be observed. $p16^{INK4a}$ is a tumour suppressor protein regarded as a biomarker for the presence of HR-HPV. As expected, high $p16^{INK4a}$ expression was observed in the tissues expressing HPV16-E7. PCNA signal showing an increase in cell proliferation in the exocervix of mice in the FVB+E_2, K14E7 and K14E7+E_2 groups compared with those in the FVB group. Arrows indicate positive signals and dotted lines indicate the basal membrane. The sections were stained with H&E; H&E-stained images and visual fields are at x40 magnification. Histopathology and immunohistochemical detection were performed as described in the Materials and methods section. PCNA, proliferating cell nuclear antigen; H&E, haematoxylin and eosin; E_2, 17β-oestradiol.

K14E7 mice was increased relative to that in the FVB mice (arrows, $p16^{INK4a}$-K14E7+E_2; Fig. 1). Finally, the expression of PCNA in the E_2-treated K14E7 mice was also detected in the basal and suprabasal layers in the hyperproliferative stratified squamous epithelium of the exocervix, consistent with the presence of proliferating cells (arrows, PCNA-K14E7+E_2; Fig. 1). All these traits are characteristic of low-grade lesions corresponding to CIN-I. Classification of cervical dysplastic lesions in 2-month-old E_2-treated K14E7 mice was determined according to the 'histopathological grading system for cervical squamous carcinogenesis in transgenic mouse' (4).

Effect of the HPV16-E7 oncoprotein and E_2 on global gene expression in the initial stages of carcinogenesis. To evaluate the global gene expression profiles in the initial stages of cancer development, 2-month-old FVB and K14E7 mice treated for 1 month with E_2 pellets were used and compared against untreated FVB (control) or K14E7 mice. The 4 groups were examined with Whole Mice Genome Oligo Microarrays using ANOVA, with a fold-change criterion of ≥1.5 and ≤-1.5 and a P-value of <0.05. In summary, it was observed that the most marked changes in gene expression occurred in the E_2-treated groups (FVB or K14E7). Compared with those in the FVB group, 685 differentially expressed genes (409 upregulated and 276 downregulated) were detected in the FVB+E_2 group, 321 differentially expressed genes (181 upregulated and 140 downregulated) were detected in the K14E7 group and 933 differentially expressed genes (554 upregulated and 379 downregulated) were detected in the K14E7+E_2 group (Fig. 2A). A Venn diagram (Fig. 2B) was constructed to identify genes that were commonly and exclusively modulated by the E7 oncoprotein and/or E_2. The comparison between the K14E7+E_2 and FVB+E_2 groups yielded 248 overlapping genes, and the comparison between the K14E7+E_2 and K14E7 groups yielded 50 overlapping genes. In total, 108 genes were overlapping among all groups. Notably, 527 (K14E7+E_2), 290 (FVB+E_2) and 124 (K14E7) genes were exclusively regulated in each group (data not shown; dropbox data).

We hypothesize that the 527 exclusively downregulated or upregulated genes in the K14E7+E_2 group that lead to carcinogenesis are regulated by the cooperation between E_2 and E7 (Fig. 2B). To identify differentially expressed genes involved in diverse cellular processes, a Gene Ontology analysis was performed using the IPA software and it was observed that several processes associated with cancer, including 'cellular movement', 'cancer' and 'cellular growth and proliferation', were mainly modified in the K14E7+E_2 group, and to a slightly lesser degree, in the FVB+E_2 group (Fig. 3), whereas genes associated with 'inflammatory response', and 'dermatological diseases and conditions', were altered in the K14E7 group. Notably, even though the K14E7+E_2 and FVB+E_2 groups shared differentially expressed genes involved in several cellular processes, the gene profile for each group was quite different (Fig. 3).

Validation of microarray data by RT-qPCR. To validate the microarray data, genes involved in different processes were

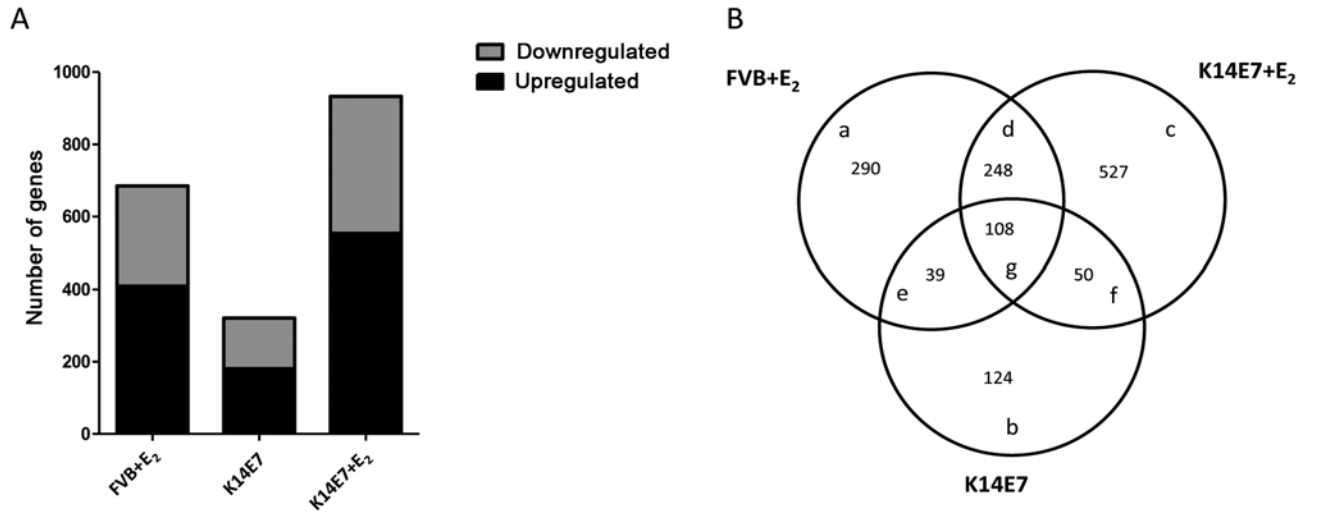

Figure 2. Global gene expression profile of the control FVB group versus the FvB+E_2, K14E7 and K14E7+E_2 groups. To determine the differentially expressed genes, a fold change of ≥1.5 and ≤−1.5, and a P-value of <0.001 were used. (A) In total, 409, 181 and 554 upregulated genes and 276, 140 and 379 downregulated genes were detected in the FVB+E_2, K14E7 and K14E7+E_2 groups, respectively, relative to the FVB group. (B) Venn diagram showing unique (a, b and c) and common (d, e, f and g) differentially expressed genes among the FVB+E_2, K14E7 and K14E7+E_2 groups. E_2, 17β-oestradiol.

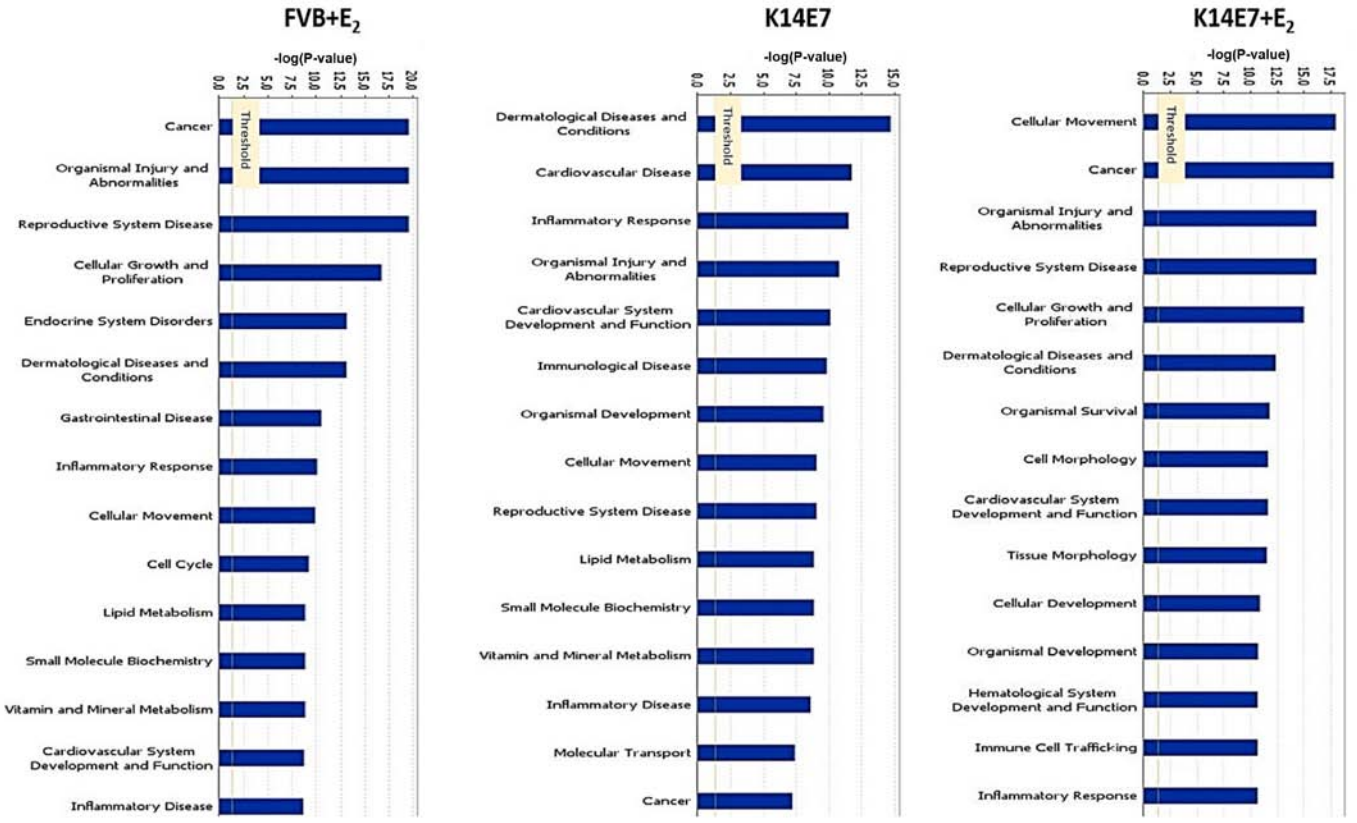

Figure 3. Gene Ontology-based biological process pathways. For each experimental group, the genes were categorized into functional groups by the IPA software. Bars indicate log(P-values), which were calculated by the IPA software corresponding to the levels of relatedness. The y-axis shows the log(P-value), and the x-axis indicates the name of the biological function. E_2, 17β-oestradiol; IPA, Ingenuity Pathway Analysis.

selected (Fig. 3) and RT-qPCR analysis was performed. A total of 15 specific genes that showed differential expression in the microarray data obtained from the K14E7+E_2 group were validated. Among the upregulated genes, cytochrome P450 family 2 subfamily e polypeptide 1 (Cyp2e1; not synergistic), glycerophosphodiester phosphodiesterase domain containing 3 (*Gdpd3*), interleukin 1 receptor type II (*Il1r2*), lecithin-retinol acyltransferase (phosphatidylcholine-retinol-O-acyltransferase) (*Lrat*), MGAT4 family member C (*Mgat4c*), natriuretic peptide type C (*Nppc*) and serine (or cysteine) peptidase inhibitor clade B member 9 [*Serpinb9b*; (PI-9); synergistic] were validated, and among the downregulated genes, eomesodermin

Table II. RT-qPCR gene validation for microarray data of 2-month-old FVB and K14E7 mice, in E_2-treated or untreated mouse groups.

	FVB+E_2 vs. FVB		K14E7 vs. FVB		K14E7+E_2 vs. FVB	
Symbol	Microarray result	RT-qPCR result	Microarray result	RT-qPCR result	Microarray result	RT-qPCR result
Gxylt2					-2.925	-4.46
Cyp2e1	2.47	-1.32	6.278	1.38	5.179	1.31
Gdpd3	-23.674	-5.99		-0.14		0.90
Il1r2	3.207	-4.33	3.187	1.64	5.934	2.64
Lrat	3.567	-5.99	2.191	-0.14	6.533	0.9
Mgat4c	4.75	-5.31			7.007	1.07
Nppc		-4.84		-0.17	9.527	0.84
Gzmb		0.05		-0.56	-2.15287	-1.08
Gzmc		-0.07		-0.87	-2.09209	-2.12
Gzmd	-2.4152	-0.45	-2.03554	-0.62	-9.45465	-5.58
Gzme		-6.83		-0.06	-2.59815	-6.66
Gzmf	-1.96428	0.24	-2.0912	0.58	-3.69359	-5.14
Gzmg	-1.84094	-1.11	-1.7933	-1.86	-3.48101	-5.42
Eomes	-1.509	-3.62		-0.38	-1.854	-0.81
Serpinb9b		-3.00		2.15	2.085	4.24

Microarrays results are presented as fold change and RT-qPCR results are presented as log (fold-change). RT-qPCR, reverse transcription-quantitative polymerase chain reaction analysis; Gzm, Granzyme; *Cyp2e1*, cytochrome P450 family 2 subfamily e polypeptide 1; *Gdpd3*, glycerophosphodiester phosphodiesterase domain containing 3; *Il1r2*, interleukin 1 receptor type II; *Lrat*, lecithin-retinol acyltransferase (phosphatidylcholine-retinol-O-acyltransferase); *Mgat4c*, MGAT4 family member C; *Nppc*, natriuretic peptide type C; *Gxylt2*, glucoside xylosyltransferase 2; *GZMB*, Granzyme B; *Eomes*, eomesodermin; *Serpinb9*, serine (or cysteine) peptidase inhibitor clade B member 9.

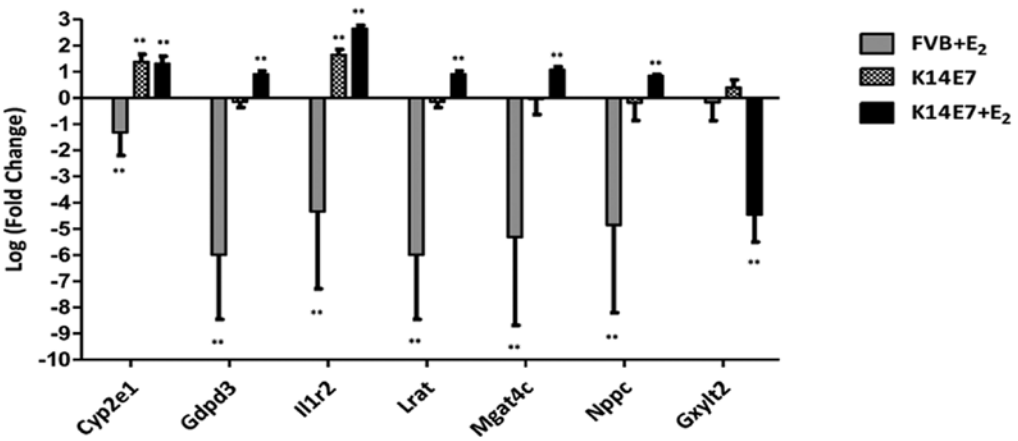

Figure 4. E_2 and the E7 oncoprotein synergistically regulate the expression of several cancer-related genes. Reverse transcription-quantitative polymerase chain reaction analysis results showed higher mRNA expression (or inhibition for *Gxylt2*) in the K14E7+E_2 group than in the untreated K14E7 group or FVB+E_2 when compared with the control group FVB (base line). Bars (relative expression) represent the mean ± standard deviation, normalized to *Gapdh* mRNA levels, from six independent experiments (**P<0.01; one-way analysis of variance with Bonferroni correction) compared with the controls (untreated FVB mice). E_2, 17β-oestradiol; *Cyp2e1*, cytochrome P450 family 2 subfamily e polypeptide 1; *Gdpd3*, glycerophosphodiester phosphodiesterase domain containing 3; *Il1r2*, interleukin 1 receptor type II; *Lrat*, lecithin-retinol acyltransferase (phosphatidylcholine-retinol-O-acyltransferase); *Mgat4c*, MGAT4 family member C; *Nppc*, natriuretic peptide type C; *Gxylt2*, glucoside xylosyltransferase 2.

(*Eomes*; not synergistic), *Gzmb, Gzmc, Gzmd, Gzme, Gzmf, Gzmg* and glucoside xylosyltransferase 2 (synergistic) were validated. The results for all the genes analysed by RT-qPCR were consistent with the microarray data; the comparative results are shown in Table II. A synergistic effect at the transcriptional level was found in 13 of the validated genes, probably as a result of interactions between E_2 and E7. Another set of genes that showed differential expression in the K14E7 group (*Cyp2e1, Il1r2, Gzmd* and *Gzmg*) and in the FVB+E_2 group (*Gdpd3, Gzmd, Gzmg* and *Eomes*) was also validated. Validation of all groups was made using FVB untreated mice as the control. The RT-qPCR results are summarized in Figs. 4-6.

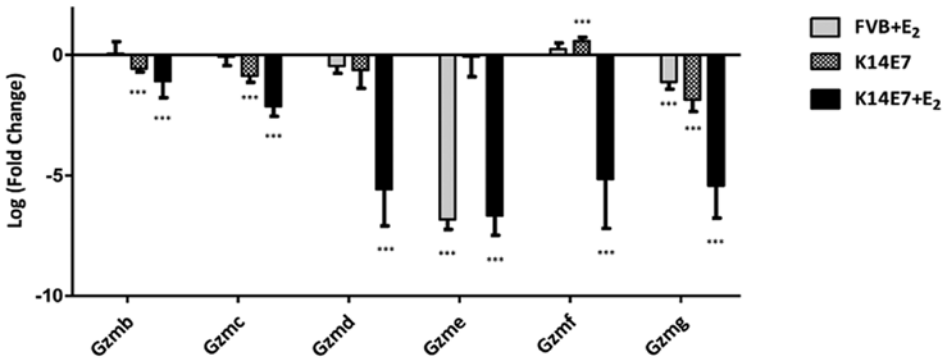

Figure 5. E_2 and the E7 oncoprotein synergistically repress the expression of the Granzyme gene family. Reverse transcription-quantitative polymerase chain reaction analysis results showed lower mRNA expression of *Gzmb, Gzmc, Gzmd, Gzme, Gzmf* and *Gzmg* in the K14E7+E_2 mice than in the untreated mice (K14E7) or treated non-transgenic mice (FVB+E_2). Bars (relative expression) represent the mean ± standard deviation, normalized to *Gapdh* mRNA levels, from six independent experiments (***P<0.001; one-way analysis of variance with Bonferroni correction) compared with the controls (untreated FVB mice). Gzm, Granzyme; E_2, 17β-oestradiol.

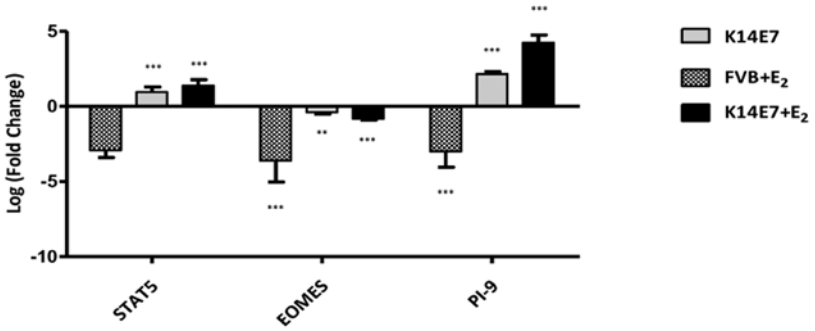

Figure 6. E_2 and the E7 oncoprotein synergistically promote the expression of Granzyme-associated transcription factors and *Serpinb9* (PI-9). Reverse transcription-quantitative polymerase chain reaction analysis results showed higher mRNA expression of PI-9 in K14E7+E_2 mice than in untreated transgenic mice (K14E7) or treated non-transgenic mice (FVB+E_2). The results show comparable repression of *Eomes* in the three groups, without a significant difference in the expression of *Stat5* in the presence of the E7 oncoprotein. Bars (relative expression) represent the mean ± standard deviation, normalized to *Gapdh* mRNA levels, from six independent experiments (***P<0.001 and **P<0.01; one-way analysis of variance with Bonferroni correction) compared with the controls (untreated FVB mice). *Eomes*, eomesodermin; *Serpinb9*, serine (or cysteine) peptidase inhibitor clade B member 9; PI-9, protease inhibitor-9; *Stat5*, signal transducer and activator of transcription 5.

Protein expression of GrB and PI-9 in the murine exocervix, as determined by immunofluorescence. To validate whether GrB and PI-9 protein expression was associated with the mRNA expression, immunofluorescence assays were performed for GrB and its inhibitor, PI-9, in tissue sections of murine exocervix obtained from the FVB, FVB+E_2, K14E7 and K14E7+E_2 groups. Consistent with the mRNA expression results, immunofluorescence assays demonstrated cytoplasmic GrB protein expression in the suprabasal and granular layers of exocervical tissues from the FVB control group (GrB-FVB; Fig. 7). For the FVB+E_2 group, high GrB expression in the hyperplasic epithelial cells of the suprabasal and granular layers of the exocervix was also found (GrB-FVB+E_2; Fig. 7). A low signal for GrB in the K14E7 group was found (GrB-K14E7; Fig. 7), and as expected, a very weak signal was observed in the K14E7+E_2 mice, indicating the downregulation of GrB at the protein level (GrB-K14E7+E_2; Fig. 7). On the other hand, also in accordance with the microarray and RT-qPCR results, the expression of PI-9 was very low in the FVB group, and PI-9 expression was not observed in the FVB+E_2 group (PI-9-FVB and PI-9-FVB+E_2; Fig. 7). Moreover, a clear cytoplasmic signal for PI-9 was observed in the basal and suprabasal layers of the cervical epithelium and the stromal tissues in the K14E7 group (PI-9-K14E7; Fig. 7), and a very high signal was observed in the basal and suprabasal layers of the epithelial tissues in the K14E7+E_2 group (PI-9-K14E7+E_2; Fig. 7).

HPV16-E7 oncoprotein inhibits GrB expression and enhances PI-9 expression in human keratinocytes. To verify the effect of the HPV16-E7 oncoprotein on human GrB and PI-9 expression, HFK cell lines transiently or stably transfected with plasmids carrying the ORF for the HPV16-E7 oncoprotein were generated. By RT-qPCR analysis, it was determined that compared with that in the HFKs transfected with empty vector, GrB expression in HFKs that were stably transfected with HPV16-E7 and exposed to UV was inhibited (Fig. 8A). PI-9 expression was upregulated by 2.0-fold when HFKs were transiently transfected with the HPV16-E7 oncoprotein ORF (Fig. 8B) and by 5.2-fold when HFKs were stably transfected (Fig. 8C). These results suggest that the HPV16-E7 oncoprotein induces PI-9 expression *in vivo* and *in vitro*. The expression of E7 was determined by RT-qPCR in stably transfected HFKs (see figure S1 available in the following Dropbox location: https://www.dropbox.com/s/h8kbqty7umkbg60/Figure%20S1.pdf?dl=0). The expression of E7 was determined by RT-qPCR in stably transfected HFKs (data not shown; dropbox data).

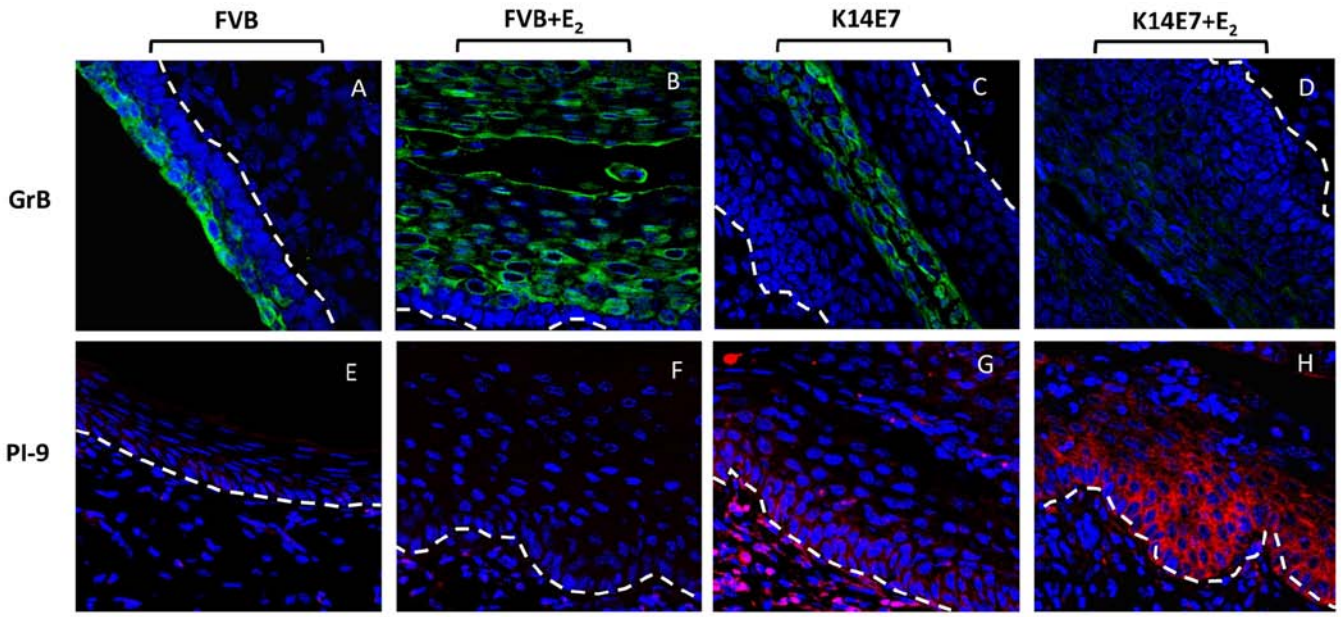

Figure 7. Immunofluorescence of GrB and PI-9 in exocervical tissues of mice. Images correspond to cross-sections of exocervical epithelium. GrB protein (green) expression is downregulated in the K14E7+E_2 group. PI-9 protein (red) is highly expressed in the cytoplasm of the K14E7+E_2 group. Nuclei were labelled with DAPI (blue). Magnification, x63. PI-9, protease inhibitor-9; GrB, Granzyme B.

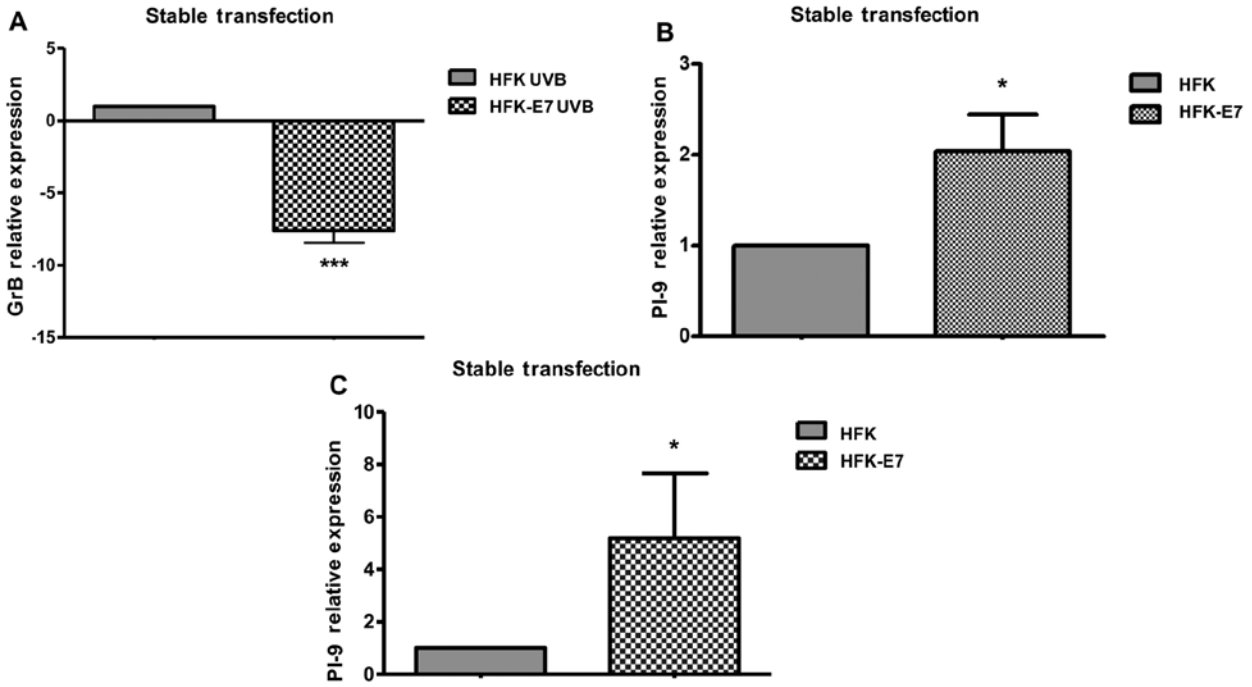

Figure 8. E7 inhibits *Gzmb* expression and enhances PI-9 expression *in vitro*. (A) Reverse transcription-quantitative polymerase chain reaction analysis results showed the inhibition of *Gzmb* mRNA expression in stably transfected HPV16-E7 HFKs. (B) The presence of HPV16-E7 corresponded to an increase in PI-9 mRNA levels in the transient transfection experiment and (C) stably transfected HFKs. Bars (relative expression) represent the mean ± standard deviation, normalized to β2-microglobulin level, from three independent experiments (*P<0.05; one-way analysis of variance with Bonferroni correction) and compared with the controls (HFKs). *Gzmb*, Granzyme B; PI-9, protease inhibitor-9; HPV, human papilloma virus type 16; HFK, human foreskin primary keratinocytes; UVC, ultraviolet C.

Discussion

HR-HPV infection and E_2 treatment increase the risk of CC development through oestrogen receptor α (6,26,27). In addition, E_2 cooperates with HPV oncogenes in mouse models to induce premalignant lesions and CC, but little is known about the molecular mechanisms by which E7 and E_2 contribute to the early stages of cervical carcinogenesis.

Global gene expression studies are of great importance in understanding various processes in human cancer (28). In the present study, global gene expression profiling was performed of cervical tissues from young (2-month-old) K14E7 and FVB

mice, which were either treated with E_2 or left untreated for 1 month to obtain a better understanding of the transcriptional events occurring in the early stages of cervical tumourigenesis. One important observation was that the profiles of genes associated with cancer were different between the FVB+E_2 and K14E7+E_2 groups (Fig. 3). Gene Ontology analysis showed that the genes relevant to 'cancer' in the FVB+E_2 group (Fig. 3) were mainly associated with cell cycle regulation and cell morphology, whereas genes in 'cancer' in the K14E7+E_2 group (Fig. 3) were particularly associated with lipid metabolism and endocrinological disorders (dropbox data). The overexpression of the genes involved in lipid metabolism in the K14E7+E_2 group is notable, as this group of mice eventually develop high-grade lesions and CC. It is known that cancer cells must reprogram their metabolic pathways to match their accelerated proliferation and survival rates (29) by changing the expression and activity of lipid metabolism-related enzymes that are directly regulated by the activity of oncogenic signals (30). Altered lipid metabolism is currently recognized as a hallmark of cancer, and the expression and activity of numerous enzymes involved in fatty acid synthesis, including ATP citrate lyase, acetyl-CoA carboxylase and fatty acid synthase (FASN), are upregulated in a number of cancer types (31). In the present study, the microarray results from the K14E7+E_2 group demonstrated overexpression of acyl-CoA synthetase bubblegum family member 1, acyl-CoA synthetase long-chain family member 1 and DDHD domain containing 1 genes, which encode enzymes involved in the synthesis of long-chain fatty acids in the FASN pathway. The upregulation of the fatty acid biosynthetic pathway starts at a relatively early stage in various types of tumours (32,33), which is consistent with the present results. Notably, the endocrine process was the second-most altered process, and it is associated with genes encoding receptors of hormonal responses, such as insulin (protein tyrosine phosphatase, non-receptor type 1), oestrogen (steroid 5 α-reductase 2, and gene regulated by oestrogen in breast cancer protein) and progesterone (progesterone receptor). This is not unexpected, as CC has been identified as a hormone-related malignancy. In experimental animal models, the incidence of neoplasia can be increased by excessive hormonal stimulation of the target organ (34). In this type of hormone-related neoplasia, the neoplasms produced are initially responsive to and dependent on hormones, but eventually, these neoplasms become autonomous (35).

In 1996, Arbeit *et al* (36) described a distinct synergism between oestrogen and the HPV oncoprotein, which was independent of the marked effect of E_2 promotion of HPV transcription of E6 and E7. A review also highlighted the presence of synergistic effects in HPV mouse models that were treated with oestrogen to induce cancer, although the full implications of this synergistic collaboration remain unclear (26). The present study observed a synergistic association between E7 and E_2 at the level transcriptional regulation, and these two factors enhanced or repressed the expression of several genes and promoted the expression of unique genes in each group of mice. Furthermore, this synergistic interaction between E7 and E_2 resulted in distinct gene expression profiles even within the same ontological processes compared with that in the groups that did not develop cancer (FVB, FVB+E_2 and K14E7). Although some of these genes have already been implicated in cancer, a number are new in the context of CC; for example, Nppc is expressed in prostate cancer (37-39), GDPD3 is overexpressed in luminal B type breast cancer (40), MGAT4C is associated with prostate cancer risk (41), IL1R2 is observed in relation to colon cancer and is associated with enhanced angiogenesis (42), and LRAT is involved in the metabolism of retinoic acid, which when overexpressed, increases the sensitivity of cells to carcinogens (43). Most notably, the synergistic effect of the HPV16-E7 oncoprotein and E_2 on the downregulation of the Granzyme gene family was observed in the present study. The expression of GrB by cytotoxic lymphocytes and natural killer cells has been known for a considerable time, but it is now accepted that GrB can also be expressed in other cell types of non-immune origin, including smooth muscle cells, keratinocytes and chondrocytes (14,44). For example, under certain circumstances, such as exposure to UVB and UVA radiation, keratinocytes can induce the expression and activation of GrB, which exerts cytotoxic activities and the capacity to degrade extracellular matrix (ECM) components, including collagen, elastin and fibronectin (13,45). Thus, the present results in the K14E7+E_2 group suggest that the early inhibition of the GrB pathway may prevent keratinocytes from acquiring several characteristics that could be disadvantageous to CC development, thereby promoting the survival of CC cells. It has been shown that the increase in endogenous GrB levels in chondrocytes and keratinocytes corresponds to the increase in the levels of apoptosis (13,46). Thus, the downregulation of GrB could prevent undesired activation of GrB, which may induce self-regulated apoptosis in cancer cells. On the other hand, GrB has non-apoptotic activities, including the degradation of ECM components, which could assist in enhancing innate immune responses (47). In this regard, it has been shown that the GrB-mediated degradation of ECM components may positively modulate signals for innate immune responses, and it has also been shown that tumour-associated ECM hampers T-cell functions (48,49). This suggests that collagen in the tumour microenvironment can be a barrier against T-cell penetration, and GrB collagen degradation may facilitate T-cell migration into the tumour (50). Finally, it has also been reported that collagen degradation can produce a chemotactic signal that attracts immune cells (51,52). Thus, GrB inhibition may aid in inhibiting or diminishing the host immune responses. Although there is the possibility that GrB downregulation can be induced by epigenetic mechanisms mediated by E7 and E_2 (53,54), there is also the possibility that the transcriptional inhibition of GrB was likely due to a decrease in the expression of specific transcription factors, including T-cell-specific T-Box transcription factor and eomesodermin (*EOMES*), which are regulated upstream by signal transducer and activator of transcription 5A (STAT5). It has been shown that these transcription factors cooperate to promote cytotoxic lymphocyte activation by inducing the expression of perforin and GrB (55). In this regard, it was found that the expression of the transcription factor *Eomes* was downregulated in the FVB+E_2, K14E7 and K14E7+E_2 groups compared with that in the FVB control group, regardless of the rise in the expression of Stat5 in the K14E7 and K14E7+E_2 groups compared with that in the FVB control group, suggesting in this case that downregulation of Eomes and GrB is independent of Stat5. Furthermore, it has previously been shown

that *Eomes* induces the expression of interferon-γ, which is important for the initiation of antiviral defence mechanisms in keratinocytes, suggesting that the inhibition of *Eomes* could also be a mechanism of immune evasion (56-58). However, there is little evidence to support that the HPV-E7-mediated downregulation of GrB observed in keratinocytes could also occur in immune cells, and if this process does occur, it may be regulated by mechanisms distinct from those regulating the downregulation of endogenous GrB in keratinocytes; for example, these mechanisms may involve soluble components (e.g., cytokines) produced by infected cells. A previous study on lung cancer cells demonstrated a reduction in the expression of GrB in cluster of differentiation 8-positive T cells in response to culture media from cancer cells, supporting the idea of an inhibitory signal for GrB expression in immune cells (59). In addition, in the K14E7+E_2 group in the present study, an increase was observed in the expression of PI-9, which is a potent inhibitor of GrB (60) and a key regulator of GrB activity. Endothelial cells, vascular smooth muscle cells and hepatocytes have the ability to express PI-9 to protect themselves from GrB-mediated cytotoxicity (61,62). Notably, oestrogens have been shown to induce PI-9 expression in hepatoblastoma cells to protect the cells from CTLs and NK cell-mediated GrB-dependent apoptosis (63). Furthermore, the exposure of MCF7 cells to oestrogens (E_2 and genistein) has been shown to increase PI-9 protein level, and at the same time, to increase the number and size of tumour spheres and to promote cell proliferation (64). In addition, PI-9 transfection experiments in HeLa and CHO cells lines have also shown that PI-9 expression aids in the evasion of cell death by lymphocytes (65,66). In addition suppression of Granzyme B initiated apoptosis in PI-9-expressing cells could contribute to immune evasion (68). The present study used *in vitro* assays to support the *in vivo* observations, which confirmed that in HPV16-E7 transfected keratinocytes, GrB expression was inhibited, while protease inhibitor-9 (PI-9) expression was robustly enhanced. There are also clinical studies in non-Hodgkin's and Hodgkin's lymphoma that support these observations (67).

In conclusion, HPV16-E7 and oestrogens (E_2) negatively regulate GrB expression and activity, and increase the expression of PI-9 in keratinocytes, indicating the possibility that GrB downregulation prevents precancerous cells from acquiring cytotoxic capacities, which may be detrimental to cancer development, and indicating that the upregulation of PI-9 may contribute to immune evasion by cancer cells. These two factors may thus be useful as predictive markers and as novel therapeutic targets during the early stages of cancer (68). Considering the results of the present study, in order to demonstrate *in vivo* that the depletion of Granzyme B or the expression of PI-9 is essential for the progression of low-grade lesions to carcinoma *in situ*, a double transgenic mouse model that expresses E7 and GrB under K14 promoter control or a double transgenic system that expresses E7 and incorporates a PI-9-knockout, could be useful. Another possible experiment would be to xenotransplant CC cells that express constitutively GrB or PI-9 in a wild-type mouse model in order to evaluate its ability to generate a tumour. Furthermore, an extended histopathological analysis of GrB and PI-9 in clinical samples of low-, medium- and high-grade lesion is necessary to establish a positive correlation with CC progression.

Acknowledgements

The authors would like to thank to Mr. Raúl Mojica (The National Institute of México City, México), Mr. Jaime Escobar-Herrera from the Department of Cellular Biology (The Centre for Research and Advanced Studies of the National Polytechnic Institute, México City, México), Mr. Ricardo Águila Guadarrama (The National Institute of Medical Sciences and Nutrition Salvador Zubirán - Health Secretary, México City, México), Dr Ricardo Gaxiola-Centeno, Dr Benjamín Chavez-Alvarez and Mr. Rafael Leyva (Unit for the Production and Experimentation of Laboratory Animals, The Centre for Research and Advanced Studies of the National Polytechnic Institute) for their excellent technical support. The authors would also like to thank the Cinvestav employees and Mr. Lauro Macías González (The Centre for Research and Advanced Studies of the National Polytechnic Institute) for providing technical support and Miss Rosa Angélica Becerril Gutiérrez, Miss Altair Munguia Torres and Mrs. Denisse Torres Hernandez (all affiliated to The Centre for Research and Advanced Studies of the National Polytechnic Institute) for their critical comments.

Funding

This study was supported by government grants from the Institute of Science and technology of Mexico City (nos. PICSA10-190 and 326/2011), from the National Council for Science and Technology (no. 168896) and from the Sectorial Funding for Research in Health and Social Security (no. 261875).

Availability of data and materials

The datasets used and/or analyzed during the current study are available from the corresponding author on reasonable request. The datasets generated during the current study are also available in the following dropbox locations: https://www.dropbox.com/s/z55z32y738s54sq/TABLE%202%20venn%20diagram%20database%20.pdf?dl=0 and https://www.dropbox.com/s/h8kbqty7umkbg60/Figure%20S1.pdf?dl=0.

Authors' contributions

JAMM and JDC performed experiments, contributed to the analysis and interpretation of the data, and were major contributors in writing the manuscript. EGV, MEAS, ROD, JBD, AMF, EAR and EMCM also performed experiments. DMV and AHM performed the microarray experiments, analysis and interpretation of the data. AÜ and HÇ achieved the E7 transfection in keratinocytes. PL developed the K14E7 transgenic mice, and participated in the writing and revision of the manuscript. PG contributed to the conception and design of the study, the data analysis and interpretation, and the writing and revision of the manuscript. All authors have read and approved the final version of the manuscript.

Ethics approval and consent to participate

All experiments and procedures were approved by the Research Unit for Laboratory Animal Care Committee

(NOM-062-ZOO-1999; Unit for the Production and Experimentation of Laboratory Animals, The Centre for Research and Advanced Studies of the National Polytechnic Institute, México City, México).

Consent for publication

Not applicable.

Competing interests

The authors declare that they have no competing interests.

References

1. zur Hausen H: Papillomaviruses in the causation of human cancers - a brief historical account. Virology 384: 260-265, 2009.
2. Ferlay J, Soerjomataram I, Dikshit R, Eser S, Mathers C, Rebelo M, Parkin DM, Forman D and Bray F: Cancer incidence and mortality worldwide: Sources, methods and major patterns in GLOBOCAN 2012. Int J Cancer 136: E359-E386, 2015.
3. Smith JS, Lindsay L, Hoots B, Keys J, Franceschi S, Winer R and Clifford GM: Human papillomavirus type distribution in invasive cervical cancer and high-grade cervical lesions: A meta-analysis update. Int J Cancer 121: 621-632, 2007.
4. Riley RR, Duensing S, Brake T, Münger K, Lambert PF and Arbeit JM: Dissection of human papillomavirus E6 and E7 function in transgenic mouse models of cervical carcinogenesis. Cancer Res 63: 4862-4871, 2003.
5. Brake T and Lambert PF: Estrogen contributes to the onset, persistence, and malignant progression of cervical cancer in a human papillomavirus-transgenic mouse model. Proc Natl Acad Sci USA 102: 2490-2495, 2005.
6. Chung SH, Wiedmeyer K, Shai A, Korach KS and Lambert PF: Requirement for estrogen receptor alpha in a mouse model for human papillomavirus-associated cervical cancer. Cancer Res 68: 9928-9934, 2008.
7. Cortés-Malagón EM, Bonilla-Delgado J, Díaz-Chávez J, Hidalgo-Miranda A, Romero-Cordoba S, Uren A, Celik H, McCormick M, Munguía-Moreno JA, Ibarra-Sierra E, *et al*: Gene expression profile regulated by the HPV16 E7 oncoprotein and estradiol in cervical tissue. Virology 447: 155-165, 2013.
8. Nickens KP, Han Y, Shandilya H, Larrimore A, Gerard GF, Kaldjian E, Patierno SR and Ceryak S: Acquisition of mitochondrial dysregulation and resistance to mitochondrial-mediated apoptosis after genotoxic insult in normal human fibroblasts: A possible model for early stage carcinogenesis. Biochim Biophys Acta 1823: 264-272, 2012.
9. Rousalova I and Krepela E: Granzyme B-induced apoptosis in cancer cells and its regulation (review). Int J Oncol 37: 1361-1378, 2010.
10. Berthou C, Michel L, Soulié A, Jean-Louis F, Flageul B, Dubertret L, Sigaux F, Zhang Y and Sasportes M: Acquisition of granzyme B and Fas ligand proteins by human keratinocytes contributes to epidermal cell defense. J Immunol 159: 5293-5300, 1997.
11. Hernandez-Pigeon H, Jean C, Charruyer A, Haure MJ, Titeux M, Tonasso L, Quillet-Mary A, Baudouin C, Charveron M and Laurent G: Human keratinocytes acquire cellular cytotoxicity under UV-B irradiation. Implication of granzyme B and perforin. J Biol Chem 281: 13525-13532, 2006.
12. Fang Y, Herrick EJ and Nicholl MB: A possible role for perforin and granzyme B in resveratrol-enhanced radiosensitivity of prostate cancer. J Androl 33: 752-760, 2012.
13. Hernandez-Pigeon H, Jean C, Charruyer A, Haure MJ, Baudouin C, Charveron M, Quillet-Mary A and Laurent G: UVA induces granzyme B in human keratinocytes through MIF: Implication in extracellular matrix remodeling. J Biol Chem 282: 8157-8164, 2007.
14. Boivin WA, Cooper DM, Hiebert PR and Granville DJ: Intracellular versus extracellular granzyme B in immunity and disease: Challenging the dogma. Lab Invest 89: 1195-1220, 2009.
15. Khan MS, Singh P, Azhar A, Naseem A, Rashid Q, Kabir MA and Jairajpuri MA: Serpin inhibition mechanism: A delicate balance between native metastable state and polymerization. J Amino Acids 2011: 606797, 2011.
16. Medema JP, de Jong J, Peltenburg LT, Verdegaal EM, Gorter A, Bres SA, Franken KL, Hahne M, Albar JP, Melief CJ, *et al*: Blockade of the granzyme B/perforin pathway through overexpression of the serine protease inhibitor PI-9/SPI-6 constitutes a mechanism for immune escape by tumors. Proc Natl Acad Sci USA 98: 11515-11520, 2001.
17. Herber R, Liem A, Pitot H and Lambert PF: Squamous epithelial hyperplasia and carcinoma in mice transgenic for the human papillomavirus type 16 E7 oncogene. J Virol 70: 1873-1881, 1996.
18. Ibarra Sierra E, Díaz Chávez J, Cortés-Malagón EM, Uribe-Figueroa L, Hidalgo-Miranda A, Lambert PF and Gariglio P: Differential gene expression between skin and cervix induced by the E7 oncoprotein in a transgenic mouse model. Virology 433: 337-345, 2012.
19. Kendziorski C, Irizarry RA, Chen KS, Haag JD and Gould MN: On the utility of pooling biological samples in microarray experiments. Proc Natl Acad Sci USA 102: 4252-4257, 2005.
20. Chabas D, Baranzini SE, Mitchell D, Bernard CC, Rittling SR, Denhardt DT, Sobel RA, Lock C, Karpuj M, Pedotti R, *et al*: The influence of the proinflammatory cytokine, osteopontin, on autoimmune demyelinating disease. Science 294: 1731-1735, 2001.
21. Kainkaryam RM, Bruex A, Gilbert AC, Schiefelbein J and Woolf PJ: poolMC: Smart pooling of mRNA samples in microarray experiments. BMC Bioinformatics 11: 299, 2010.
22. Livak KJ and Schmittgen TD: Analysis of relative gene expression data using real-time quantitative PCR and the 2(-Delta Delta C(T)) Method. Methods 25: 402-408, 2001.
23. McLaughlin-Drubin ME, Crum CP and Münger K: Human papillomavirus E7 oncoprotein induces KDM6A and KDM6B histone demethylase expression and causes epigenetic reprogramming. Proc Natl Acad Sci USA 108: 2130-2135, 2011.
24. McLaughlin-Drubin ME, Park D and Munger K: Tumor suppressor $p16^{INK4A}$ is necessary for survival of cervical carcinoma cell lines. Proc Natl Acad Sci USA 110: 16175-16180, 2013.
25. Yim EK and Park JS: Biomarkers in cervical cancer. Biomark Insights 1: 215-225, 2007.
26. Chung SH, Franceschi S and Lambert PF: Estrogen and ERalpha: Culprits in cervical cancer? Trends Endocrinol Metab 21: 504-511, 2010.
27. den Boon JA, Pyeon D, Wang SS, Horswill M, Schiffman M, Sherman M, Zuna RE, Wang Z, Hewitt SM, Pearson R, *et al*: Molecular transitions from papillomavirus infection to cervical precancer and cancer: Role of stromal estrogen receptor signaling. Proc Natl Acad Sci USA 112: E3255-E3264, 2015.
28. Dozmorov MG, Giles CB and Wren JD: Predicting gene ontology from a global meta-analysis of 1-color microarray experiments. BMC Bioinformatics 12 (Suppl 10): S14, 2011.
29. Cairns RA, Harris IS and Mak TW: Regulation of cancer cell metabolism. Nat Rev Cancer 11: 85-95, 2011.
30. Zhang F and Du G: Dysregulated lipid metabolism in cancer. World J Biol Chem 3: 167-174, 2012.
31. Menendez JA and Lupu R: Fatty acid synthase and the lipogenic phenotype in cancer pathogenesis. Nat Rev Cancer 7: 763-777, 2007.
32. Röhrig F and Schulze A: The multifaceted roles of fatty acid synthesis in cancer. Nat Rev Cancer 16: 732-749, 2016.
33. Baenke F, Peck B, Miess H and Schulze A: Hooked on fat: The role of lipid synthesis in cancer metabolism and tumour development. Dis Model Mech 6: 1353-1363, 2013.
34. Henderson BE, Ross RK, Pike MC and Casagrande JT: Endogenous hormones as a major factor in human cancer. Cancer Res 42: 3232-3239, 1982.
35. Furth J: A meeting of ways in cancer research: Thoughts on the evolution and nature of neoplasms. Cancer Res 19: 241-258, 1959.
36. Arbeit JM, Howley PM and Hanahan D: Chronic estrogen-induced cervical and vaginal squamous carcinogenesis in human papillomavirus type 16 transgenic mice. Proc Natl Acad Sci USA 93: 2930-2935, 1996.
37. Nielsen SJ, Gøtze JP, Jensen HL and Rehfeld JF: ProCNP and CNP are expressed primarily in male genital organs. Regul Pept 146: 204-212, 2008.
38. Nielsen SJ, Iversen P, Rehfeld JF, Jensen HL and Goetze JP: C-type natriuretic peptide in prostate cancer. APMIS 117: 60-67, 2009.
39. Scotland RS, Ahluwalia A and Hobbs AJ: C-type natriuretic peptide in vascular physiology and disease. Pharmacol Ther 105: 85-93, 2005.

40. Grinde MT, Skrbo N, Moestue SA, Rødland EA, Borgan E, Kristian A, Sitter B, Bathen TF, Børresen-Dale AL, Mælandsmo GM, *et al*: Interplay of choline metabolites and genes in patient-derived breast cancer xenografts. Breast Cancer Res 16: R5, 2014.
41. Demichelis F, Setlur SR, Banerjee S, Chakravarty D, Chen JY, Chen CX, Huang J, Beltran H, Oldridge DA, Kitabayashi N, *et al*: Identification of functionally active, low frequency copy number variants at 15q21.3 and 12q21.31 associated with prostate cancer risk. Proc Natl Acad Sci USA 109: 6686-6691, 2012.
42. Mar AC, Chu CH, Lee HJ, Chien CW, Cheng JJ, Yang SH, Jiang JK and Lee TC: Interleukin-1 receptor type 2 acts with c-Fos to enhance the expression of interleukin-6 and vascular endothelial growth factor A in colon cancer cells and induce angiogenesis. J Biol Chem 290: 22212-22224, 2015.
43. Amann PM, Czaja K, Bazhin AV, Rühl R, Eichmüller SB, Merk HF and Baron JM: LRAT overexpression diminishes intracellular levels of biologically active retinoids and reduces retinoid antitumor efficacy in the murine melanoma B16F10 cell line. Skin Pharmacol Physiol 28: 205-212, 2015.
44. Hiebert PR and Granville DJ: Granzyme B in injury, inflammation, and repair. Trends Mol Med 18: 732-741, 2012.
45. Provenzano PP, Inman DR, Eliceiri KW, Knittel JG, Yan L, Rueden CT, White JG and Keely PJ: Collagen density promotes mammary tumor initiation and progression. BMC Med 6: 11, 2008.
46. Saito S, Murakoshi K, Kotake S, Kamatani N and Tomatsu T: Granzyme B induces apoptosis of chondrocytes with natural killer cell-like cytotoxicity in rheumatoid arthritis. J Rheumatol 35: 1932-1943, 2008.
47. Parkinson LG, Toro A, Zhao H, Brown K, Tebbutt SJ and Granville DJ: Granzyme B mediates both direct and indirect cleavage of extracellular matrix in skin after chronic low-dose ultraviolet light irradiation. Aging Cell 14: 67-77, 2015.
48. Meyaard L: The inhibitory collagen receptor LAIR-1 (CD305). J Leukoc Biol 83: 799-803, 2008.
49. Vesely MD, Kershaw MH, Schreiber RD and Smyth MJ: Natural innate and adaptive immunity to cancer. Annu Rev Immunol 29: 235-271, 2011.
50. Salmon H, Franciszkiewicz K, Damotte D, Dieu-Nosjean MC, Validire P, Trautmann A, Mami-Chouaib F and Donnadieu E: Matrix architecture defines the preferential localization and migration of T cells into the stroma of human lung tumors. J Clin Invest 122: 899-910, 2012.
51. Sorokin L: The impact of the extracellular matrix on inflammation. Nat Rev Immunol 10: 712-723, 2010.
52. Weathington NM, van Houwelingen AH, Noerager BD, Jackson PL, Kraneveld AD, Galin FS, Folkerts G, Nijkamp FP and Blalock JE: A novel peptide CXCR ligand derived from extracellular matrix degradation during airway inflammation. Nat Med 12: 317-323, 2006.
53. Jadhav RR, Ye Z, Huang RL, Liu J, Hsu PY, Huang YW, Rangel LB, Lai HC, Roa JC, Kirma NB, *et al*: Genome-wide DNA methylation analysis reveals estrogen-mediated epigenetic repression of metallothionein-1 gene cluster in breast cancer. Clin Epigenetics 7: 13, 2015.
54. Laurson J, Khan S, Chung R, Cross K and Raj K: Epigenetic repression of E-cadherin by human papillomavirus 16 E7 protein. Carcinogenesis 31: 918-926, 2010.
55. McLane LM, Banerjee PP, Cosma GL, Makedonas G, Wherry≈EJ, Orange JS and Betts MR: Differential localization of T-bet and Eomes in CD8 T cell memory populations. J Immunol 190: 3207-3215, 2013.
56. Fukuoka N, Harada M, Nishida A, Ito Y, Shiota H and Kataoka T: Eomesodermin promotes interferon-γ expression and binds to multiple conserved noncoding sequences across the Ifng locus in mouse thymoma cell lines. Genes Cells 21: 146-162, 2016.
57. Banno T, Adachi M, Mukkamala L and Blumenberg M: Unique keratinocyte-specific effects of interferon-gamma that protect skin from viruses, identified using transcriptional profiling. Antivir Ther 8: 541-554, 2003.
58. Black AP, Ardern-Jones MR, Kasprowicz V, Bowness P, Jones L, Bailey AS and Ogg GS: Human keratinocyte induction of rapid effector function in antigen-specific memory $CD4^+$ and $CD8^+$ T cells. Eur J Immunol 37: 1485-1493, 2007.
59. Soriano C, Mukaro V, Hodge G, Ahern J, Holmes M, Jersmann H, Moffat D, Meredith D, Jurisevic C, Reynolds PN, *et al*: Increased proteinase inhibitor-9 (PI-9) and reduced granzyme B in lung cancer: Mechanism for immune evasion? Lung Cancer 77: 38-45, 2012.
60. Bird CH, Sutton VR, Sun J, Hirst CE, Novak A, Kumar S, Trapani JA and Bird PI: Selective regulation of apoptosis: The cytotoxic lymphocyte serpin proteinase inhibitor 9 protects against granzyme B-mediated apoptosis without perturbing the Fas cell death pathway. Mol Cell Biol 18: 6387-6398, 1998.
61. Buzza MS, Hirst CE, Bird CH, Hosking P, McKendrick J and Bird PI: The granzyme B inhibitor, PI-9, is present in endothelial and mesothelial cells, suggesting that it protects bystander cells during immune responses. Cell Immunol 210: 21-29, 2001.
62. Barrie MB, Stout HW, Abougergi MS, Miller BC and Thiele DL: Antiviral cytokines induce hepatic expression of the granzyme B inhibitors, proteinase inhibitor 9 and serine proteinase inhibitor 6. J Immunol 172: 6453-6459, 2004.
63. Jiang X, Orr BA, Kranz DM and Shapiro DJ: Estrogen induction of the granzyme B inhibitor, proteinase inhibitor 9, protects cells against apoptosis mediated by cytotoxic T lymphocytes and natural killer cells. Endocrinology 147: 1419-1426, 2006.
64. Lauricella M, Carlisi D, Giuliano M, Calvaruso G, Cernigliaro C, Vento R and D'Anneo A: The analysis of estrogen receptor-α positive breast cancer stem-like cells unveils a high expression of the serpin proteinase inhibitor PI-9: Possible regulatory mechanisms. Int J Oncol 49: 352-360, 2016.
65. Cunningham TD, Jiang X and Shapiro DJ: Expression of high levels of human proteinase inhibitor 9 blocks both perforin/granzyme and Fas/Fas ligand-mediated cytotoxicity. Cell Immunol 245: 32-41, 2007.
66. Deisting W, Raum T, Kufer P, Baeuerle PA and Münz M: Impact of diverse immune evasion mechanisms of cancer cells on T cells engaged by EpCAM/CD3-bispecific antibody construct AMG 110. PLoS One 10: e0141669, 2015.
67. Bladergroen BA, Meijer CJ, ten Berge RL, Hack CE, Muris JJ, Dukers DF, Chott A, Kazama Y, Oudejans JJ, van Berkum O, *et al*: Expression of the granzyme B inhibitor, protease inhibitor 9, by tumor cells in patients with non-Hodgkin and Hodgkin lymphoma: A novel protective mechanism for tumor cells to circumvent the immune system? Blood 99: 232-237, 2002.
68. Fritsch K, Finke J and Grüllich C: Suppression of granzyme B activity and caspase-3 activation in leukaemia cells constitutively expressing the protease inhibitor 9. Ann Hematol 92: 1603-1609, 2013.